Dynamics of microring resonator modulators

Wesley D. Sacher and Joyce K. S. Poon

Department of Electrical and Computer Engineering and Institute for Optical Sciences, University of Toronto, 10 King's College Rd., Toronto, Ontario, M5S 3G4, Canada.

wesley.sacher@utoronto.ca, joyce.poon@utoronto.ca

Abstract: A dynamic model for the transmission of a microring modulator based on changes in the refractive index, loss, or waveguide-ring coupling strength is derived to investigate the limitations to the intensity modulation bandwidth. Modulation bandwidths approaching the free spectral range frequency are possible if the waveguide-ring coupling strength is varied, rather than the refractive index or loss of the ring. The results illustrate that via controlled coupling, resonant modulators with high quality factors can be designed to operate at frequencies much larger than the resonator linewidth.

OCIS codes: (230.5750) Resonators; (230.4110) Modulators; (130.3120) Integrated optics devices.

References and links

1. P. Rabiei, W. H. Steier, C. Zhang, and L. R. Dalton, "Polymer micro-ring filters and modulators," J. Lightwave Technol. **20**, 1968–1975 (2002).
2. A. Guarino, G. Poberaj, D. Rezzonico, R. Degl'Innocenti, and P. Gunter, "Electrooptically tunable microring resonators in lithium niobate," Nature Photonics **1**, 407 – 410 (2007).
3. Q. F. Xu, B. Schmidt, S. Pradhan, and M. Lipson, "Micrometre-scale silicon electro-optic modulator," Nature **435**, 325–327 (2005).
4. Y. Vlasov, W. M. J. Green, and F. Xia, "High-throughput silicon nanophotonic wavelength-insensitive switch for on-chip optical networks," Nature Photonics **2**, 242–246 (2008).
5. T. A. Ibrahim, V. Van, and P.-T. Ho, "All-optical time-division demultiplexing and spatial pulse routing with a GaAs/AlGaAs microring resonator," Opt. Lett. **27**, 803–805 (2002).
6. D. G. Rabus, M. Hamacher, U. Troppenz, and H. Heidrich, "High-Q channel-dropping filters using ring resonators with integrated SOAs," IEEE Photon. Technol. Lett. **14**, 1442–1444 (2002).
7. T. Sadagopan, S. J. Choi, S. J. Choi, K. Djordjev, and P. D. Dapkus, "Carrier-induced refractive index changes in InP-based circular microresonators for low-voltage high-speed modulation," IEEE Photon. Technol. Lett. **17**, 414–416 (2005).
8. L. Zhang, J.-Y. Yang, M. Song, Y. Li, B. Zhang, R. G. Beausoleil, and A. E. Willner, "Microring-based modulation and demodulation of DPSK signal," Opt. Express **15**, 11,564–11,569 (2007).
9. I. L. Gheorma and R. M. Osgood, "Fundamental limitations of optical resonator based high-speed EO modulators," J. Lightwave Technol. **14**, 795–797 (2002).
10. K. Djordjev, S.-J. Choi, S.-J. Choi, and P. D. Dapkus, "Active semiconductor microdisk devices," J. Lightwave Technol. **20**, 105–113 (2002).
11. A. Yariv, "Universal relations for coupling of optical power between microresonators and dielectric waveguides," Electron. Lett. **36**, 321–322 (2000).
12. J. M. Choi, R. K. Lee, and A. Yariv, "Control of critical coupling in a ring resonator-fiber configuration: application to wavelength-selective switching, modulation, amplification, and oscillation," Opt. Lett. **26**, 1236–1238 (2001).
13. B. Bortnik, Y.-C. Hung, H. Tazawa, J. Luo, A. K.-Y. Jen, W. H. Steier, and H. R. Fetterman, "Electrooptic polymer ring resonator modulation up to 165 GHz," IEEE J. Sel. Top. Quantum Electron. **13**, 104 – 110 (2007).
14. B. Crosignani and A. Yariv, "Time-dependent analysis of a fiber-optic passive-loop resonator," Opt. Lett. **11**, 251–253 (1986).

#100170 - $15.00 USD Received 14 Aug 2008; revised 11 Sep 2008; accepted 16 Sep 2008; published 19 Sep 2008

15. D. Chen, H. R. Fetterman, A. Chen, W. H. Steier, L. R. Dalton, W. Wang, and Y. Shi, "Demonstration of 110 GHz electro-optic polymer modulators," Appl. Phys. Lett. **70**, 3335–3337 (1997).
16. M. Lee, H. E. Katz, C. Erben, D. M. Gill, P. Gopalan, J. D. Heber, and D. J. McGee, "Broadband modulation of light by using an electro-optic polymer," Science **298**, 1401–1403 (2002).
17. A. Yariv, "Critical coupling and its control in optical waveguide-ring resonator systems," IEEE Photon. Technol. Lett. **14**, 483–485 (2002).
18. W. M. J. Green, R. K. Lee, G. A. DeRose, A. Scherer, and A.Yariv, "Hybrid InGaAsP-InP Mach-Zehnder racetrack resonator for thermooptic switching and coupling control," Opt. Express **13**, 1651–1659 (2005).
19. C. Li, L. Zhou, and A. W. Poon, "Silicon microring carrier-injection-based modulators/switches with tunable extinction ratios and OR-logic switching by using waveguide cross-coupling," Opt. Express **15**, 5069–5076 (2007).
20. L. Zhou and A. W. Poon, "Electrically reconfigurable silicon microring resonator-based filter with waveguide-coupled feedback," Opt. Express **15**, 9194–9204 (2007).
21. W. M. J. Green, M. J. Rooks, L. Sekaric, and Y. A. Vlasov, "Optical modulation using anti-crossing between paired amplitude and phase resonators," Opt. Express **15**, 17264–17272 (2007).
22. Y. Li, L. Zhang, M. Song, B. Zhang, J. Y. Yang, R. G. Beausoleil, A. E. Willner, and P. D. Dapkus, "Coupled-ring-resonator-based silicon modulator for enhanced performance," Opt. Express **16**, 13342–13348 (2008).

1. Introduction

Because of their compact sizes and potential for low power consumption, microring resonator modulators have attracted significant scientific and technological interest in recent years. A waveguide-coupled microring resonator, such as the one shown in Fig. 1, can be used as an amplitude or phase modulator. Amplitude modulators based on microrings have been demonstrated in polymeric [1], lithium niobate [2], silicon [3, 4], and compound semiconductor materials [5, 6, 7], with typical modulation rates in the range of tens of gigahertz. Microring phase modulators have also been demonstrated, but less commonly than amplitude modulators [8].

Thus far, many discussions on resonator modulators have relied on static, steady-state models and come to the conclusion that the modulation rate is limited by the resonator quality factor (Q) [1, 9, 10]. However, to completely understand the limitations of these devices, a fully dynamical analysis of the modulation is required. In this article, we present a dynamical analysis of ring resonator modulators to show that, contrary to general expectations, the Q factor need not impose a limitation on modulation rates.

The resonator modulator configuration we shall focus on is shown in Fig. 1: a continuous-wave (CW) incoming optical wave is modulated by varying certain physical parameters of the microring resonator. In principle, three parameters can be varied to achieve modulation: 1. the refractive index of the microring, 2. the loss of the microring, and 3. the coupling strength between the microring and the bus waveguide. Experimentally, most demonstrations of microring modulators have relied on the modulation of the index of the microring waveguide [1, 2, 3, 7].

This article is organized as follows. In Section 2, we will describe a time-dependent model

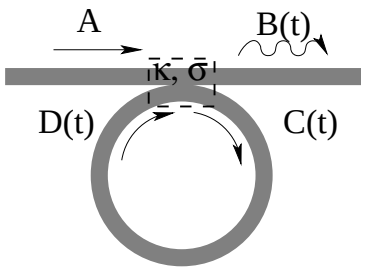

Fig. 1. Schematic of a ring resonator modulator.

#100170 - $15.00 USD Received 14 Aug 2008; revised 11 Sep 2008; accepted 16 Sep 2008; published 19 Sep 2008

of the microring. We will then analyze the modulation characteristics of the microring when the loss (Section 3), index (Section 4), and waveguide-ring coupling (Section 5), is varied. To gain a better intuitive understanding of the resonator modulation characteristics, we will derive small signal limits from our complete model. Our dynamical model reveals that to achieve modulation rates beyond that imposed by the resonator Q, the coupling coefficient, not the refractive index or loss of the ring resonator waveguide, should be modulated.

2. Time-dependent microring transmission

In this section, we shall derive a general expression to describe the dynamics of the microring modulator illustrated in Fig. 1. The electric field at the various locations in Fig. 1 can be expressed as $E_\xi(t) = \xi(t)\exp(i\omega_0 t)$, where $\xi = B$, C, D and is a slowly varying amplitude, and ω_0 is the frequency of the input optical wave. The input amplitude is constant, such that $E_A(t) = A\exp(i\omega_0 t)$.

In the presence of an index and/or loss modulation, the phase-shift, ϕ, and attenuation, a, experienced by a circulating wave at a frequency ω after each round-trip in the resonator can be expressed by

$$\phi(t,\omega) = \omega\tau + \frac{\omega}{n}\int_{t-\tau}^{t} \eta(t')\mathrm{d}t', \tag{1a}$$

$$a(t) = a_0 + \frac{1}{\tau}\int_{t-\tau}^{t} \gamma(t')\mathrm{d}t, \tag{1b}$$

where $\tau = nL/c$ is the resonator round-trip time, n is the effective index, L is the ring circumference, and

$$n_i(t) = n + \eta(t), \tag{2a}$$

$$a_i(t) = a + \gamma(t) \tag{2b}$$

are the instantaneous refractive index and attenuation coefficient respectively.

Each frequency component of $C(t)$ propagates around the ring and experiences a different phase-shift, such that

$$D(t) = \frac{a(t)}{2\pi}\int_{-\infty}^{\infty} \tilde{C}(\Omega)\exp[-i\phi(t,\omega)]\mathrm{d}\Omega, \tag{3}$$

where $\Omega = \omega - \omega_0$ and $\tilde{C}(\Omega)$ is the Fourier transform of $C(t)$. To simplify Eq. (3), we assume that $\phi(t,\omega) \approx \phi(t,\omega_0) + \Omega\tau$, which is equivalent to approximating that the change in the phase-shift of each frequency component circulating in the resonator due to the index modulation, the $\eta(t)$ term in Eq. (1a), is the same or is negligible compared to $\Omega\tau$. This assumption is reasonable since typical index changes are on the order of $\sim 10^{-3}$. With this approximation, Eq. (3) simplifies to

$$D(t) = a(t)\exp[-i\phi(t,\omega_0)]C(t-\tau). \tag{4}$$

To analyze the fundamental limitations imposed by the device structure itself, we remove any material specific dependencies and neglect the coupling between the refractive index and absorption through the Kramers-Kronig relations. This simplifying assumption allows us to isolate the effect of each resonator parameter. In this approximation, the instantaneous field amplitudes are

$$B(t) = \sigma(t)A + i\kappa(t)a(t)\exp[-i\phi(t)]C(t-\tau), \tag{5a}$$

$$i\kappa(t)C(t) = \sigma(t)B(t) - A, \tag{5b}$$

where $\phi(t) = \phi(t,\omega_0)$ and $\kappa(t)$ and $\sigma(t)$ are the resonator-waveguide coupling and transmission coefficients, and $\sigma^2(t) + \kappa^2(t) = 1$ for a lossless coupler.

#100170 - $15.00 USD Received 14 Aug 2008; revised 11 Sep 2008; accepted 16 Sep 2008; published 19 Sep 2008

Equation (5) gives steady-state or static transmission [11]:

$$T_{ss} \equiv \frac{B}{A} = \frac{\sigma - a\exp(-i\phi)}{1 - a\sigma\exp(-i\phi)}. \tag{6a}$$

$$|T_{ss}|^2 = \frac{\sigma^2 + a^2 - 2a\sigma\cos(\phi)}{1 + a^2\sigma^2 - 2a\sigma\cos(\phi)}. \tag{6b}$$

We observe that a and σ are interchangeable in $|T_{ss}|^2$. The situation when $\sigma = a$ is referred to as *critical coupling*. At critical coupling, the wave in the bus waveguide destructively interferes with the wave coupled out of the ring to result in zero transmission [11, 12]. To have complete extinction of the input wave, the modulator must thus operate near the critical coupling condition. Moreover, to use small changes in the index, loss, or coupling to cause large changes in the output intensity, the Q of the resonator must be high (a, $\sigma \approx 1$), so that a circulating wave can, in essence, experience any small changes in device parameters many times before being dissipated.

For a general expression of the dynamical transmission, $T(t)$, we eliminate $C(t)$ in Eq. (5), to arrive at

$$T(t) \equiv \frac{B(t)}{A} = \sigma(t) + \frac{\kappa(t)}{\kappa(t-\tau)} a(t)\exp[-i\phi(t)][\sigma(t-\tau)T(t-\tau) - 1]. \tag{7}$$

If $a(t)$, $\kappa(t)$, $\sigma(t)$, and $\phi(t)$ are periodic with a period equal to τ, then $T(t)$ is equal to T_{ss} but with the static parameters replaced by their time-dependent counterparts. Sinusoidally periodic modulation of the refractive index of ring resonators at the free spectral range (FSR) has been recently demonstrated in electro-optic polymers [13]. However, to solve Eq. (7) for general forms of modulation, we can express it as a Fredholm integral equation of the second kind, which possesses a Neumann series solution [14]. The Fredholm integral equation form of Eq. (7) is

$$\begin{aligned} T(t) = \sigma(t) - \frac{\kappa(t)}{\kappa(t-\tau)} a(t)\exp[-i\phi(t)] + \\ \int_{-\infty}^{\infty} \frac{\kappa(t'+\tau)}{\kappa(t')} a(t'+\tau)\sigma(t')\exp[-i\phi(t'+\tau)]\delta[t' - (t-\tau)]T(t')\mathrm{d}t'. \end{aligned} \tag{8}$$

In the following sections, we will use the Neumann series solution of Eq. (8) to model the modulation response of the microring resonator.

3. Loss modulation

We first consider the case of loss modulation, where $a(t)$ varies in time, but ϕ, σ, and κ are constant. The solution of Eq. (8) for the transmission with loss modulation, $T_a(t)$, is

$$T_a(t) = \sigma - a(t)\mathrm{e}^{-i\phi} + \sum_{n=1}^{\infty} \sigma^n \mathrm{e}^{-in\phi} \left[\sigma - a(t-n\tau)\mathrm{e}^{-i\phi}\right] \prod_{m=0}^{n-1} a(t-m\tau). \tag{9}$$

The first two terms in the above equation are the "instantaneous" response of the resonator, while the summation represents the "memory" effect of the resonator or the modulation prior to time t. Each prior round-trip is weighted by $\sigma\mathrm{e}^{-i\phi}$, so that for high Q resonators, a large number of terms in the summation will be significant to $T_a(t)$.

Equation (9) can account for arbitrary loss modulation in both magnitude and time, and, in general, must be solved numerically. However, to gain an intuition of the modulation characteristics, we can derive a small signal approximation to Eq. (9).

#100170 - $15.00 USD Received 14 Aug 2008; revised 11 Sep 2008; accepted 16 Sep 2008; published 19 Sep 2008

3.1. Small-signal approximation

We begin by considering a sinusoidal loss modulation of the form $a(t) = a_0 + a' \cos(\Omega_m t)$, where Ω_m is the modulation frequency, and $a'/a_0 \ll 1$. The Fourier transform of $a(t)$ is

$$\tilde{a}(\Omega) = a_0 \delta(\Omega) + \frac{a'}{2}[\delta(\Omega - \Omega_m) + \delta(\Omega - \Omega_m)]. \tag{10}$$

Substituting Eq. (10) into the Fourier transform of Eq. (7), gives

$$\begin{aligned} &\tilde{T}_a(\Omega)\left[1 - a_0\sigma e^{-i(\phi+\Omega\tau)}\right] - \frac{a'}{2}\sigma e^{-i(\phi+\Omega\tau)}\left[\tilde{T}_a(\Omega-\Omega_m)e^{i\Omega_m\tau} + \tilde{T}_a(\Omega+\Omega_m)e^{-i\Omega_m\tau}\right] \\ &\quad = (\sigma - a_0 e^{-i\phi})\delta(\Omega) - \frac{a'}{2}e^{-i\phi}\left[\delta(\Omega-\Omega_m) + \delta(\Omega+\Omega_m)\right], \end{aligned} \tag{11}$$

where $\tilde{T}_a(\Omega)$ is the Fourier transform of $T_a(t)$. Since we consider a sinusoidal modulation, $\tilde{T}_a(\Omega)$ consists only of the $\Omega = 0$ component and the harmonics of Ω_m.

We solve $\tilde{T}_a(\Omega)$ order by order in a'. We obtain an approximate solution by keeping only the terms up to $O(a')$ to find that

$$\tilde{T}_a(0) = \frac{\sigma - a_0 e^{-i\phi}}{1 - a_0\sigma e^{-i\phi}}\delta(0), \tag{12}$$

which is simply the steady-state transmission coefficient, and

$$\tilde{T}_a(\Omega_m) = \frac{a'}{2}\frac{e^{-i\phi}[\sigma\tilde{T}_a(0) - \delta(0)]}{1 - \sigma a_0 e^{-i(\phi+\Omega_m\tau)}} \tag{13a}$$

$$\tilde{T}_a(-\Omega_m) = \frac{a'}{2}\frac{e^{-i\phi}[\sigma\tilde{T}_a(0) - \delta(0)]}{1 - \sigma a_0 e^{-i(\phi-\Omega_m\tau)}}. \tag{13b}$$

We can neglect the higher harmonic terms since they are of higher orders of a'. Eqs. (12) and (13) show that when the input wave is near resonance so that $\exp(-i\phi) \approx 1$ and the modulation amplitude is small, the output intensity of the ring resonator is sinusoidal with the same frequency as the loss modulation but with a constant offset determined by the static response of the resonator. Eqs. (12) and (13) can also be used to study the distortion of a signal and the linearity of the modulator by evaluating the relative magnitudes and phases of $\tilde{T}_a(\pm\Omega_m)$ and $\tilde{T}_a(0)$.

Next, we will use Eqs. (12) and (13) to determine the modulation depth as a function of Ω_m. The modulation depth of a signal is defined as

$$\Delta = \frac{f(t)_{max} - f(t)_{min}}{f(t)_{max} + f(t)_{min}}, \tag{14}$$

where $f(t)_{max}$ and $f(t)_{min}$ are the maximum and minimum amplitudes of the signal. Comparing the Fourier transform of a sinusoidally modulated signal with Eq. (14), we find, after some algebra, that

$$\Delta = 2\left|\frac{\tilde{T}^*(-\Omega_m)}{\tilde{T}^*(0)} + \frac{\tilde{T}(\Omega_m)}{\tilde{T}(0)}\right|, \tag{15}$$

where $\tilde{T}(\Omega)$ is the Fourier transform of $T(t)$.

For loss modulation, substituting Eqs. (12) and (13) into Eq. (15), the modulation depth, Δ_a, is

$$\Delta_a = 2a'(1-\sigma^2)\left|\frac{\sigma\cos\phi - a_0 + \sigma a_0 e^{-i\Omega_m\tau}(a_0\cos\phi - \sigma)}{(a_0^2 + \sigma^2 - 2a_0\sigma\cos\phi)(1 + a_0^2\sigma^2 e^{-i2\Omega_m\tau} - 2a_0\sigma\cos\phi e^{-i\Omega_m\tau})}\right|. \tag{16}$$

#100170 - $15.00 USD Received 14 Aug 2008; revised 11 Sep 2008; accepted 16 Sep 2008; published 19 Sep 2008

For $\Omega_m\tau \ll 1$, Eq. (16) shows that the modulation depth decreases with increasing modulation frequency. By taking the derivative of Δ_a with respect to $\Omega_m\tau$, we find that for a, $\sigma \approx 1$, there exists a special condition when the modulation depth is maximum: $\phi + \Omega_m\tau \approx 2p\pi$, where p is an integer, i.e. when one of the sideband frequencies is on resonance. We shall refer to this situation as a *modulation resonance*. The output distortion when the modulator operates close to a modulation resonance is dictated by the relative amplitudes and phase of the resonant and non-resonant sidebands.

When the input wavelength is on resonance, for $\Omega_m\tau \ll 1$, the modulation depth simplifies to

$$\Delta_{a,res} = 2a'\frac{(1-\sigma^2)}{|\sigma - a_0|}\left[\frac{1}{(1-a_0\sigma)^2 + a_0\sigma(\Omega_m\tau)^2}\right]^{\frac{1}{2}}, \tag{17}$$

with a 3 dB roll-off at a frequency

$$\Omega_{a,\mathrm{3dB},res} = \frac{1-a_0\sigma}{\tau}\sqrt{\frac{3}{a_0\sigma}}. \tag{18}$$

$\Omega_{a,\mathrm{3dB},res}$ is higher for lower Q resonators with smaller values of a_0 and σ. Therefore, for loss modulated microrings, the modulation bandwidth is limited by the resonator Q.

3.2. Numerical results

In this section, we compare our small signal approximation results with the exact Neumann series solution. For all calculations in this work, we take the ring radius to be 10μm and the waveguide index to be $n = 3$, resulting in a round-trip time of 0.628 ps. For the summation in the Neumann series [Eq. (9)], we include terms up to $O(10^{-5})$.

Figure 2 shows the modulation depth as a function of Ω_m calculated using the small signal approximation, Eq. (17), and the exact expression, Eq. (9), when the loss of the microring is modulated between 2 dB/cm and 5 dB/cm ($a_0 = 0.9975$, $a' = 0.0011$) while $\sigma = 0.9928$. The 3 dB roll-off frequency is 4.3 GHz, in good agreement with Eq. (18). Figure 2(b) shows the presence of the modulation resonance when the input wavelength is detuned from resonance by f_m. The ratio between the modulation resonance and $\Delta_a(\Omega_m = 0)$ is larger for an input wavelength that is greater detuned from resonance. As evidenced by the figures, there is good agreement between the small signal approximation and the exact equation at frequencies below the modulation resonance. At higher frequencies, higher order (harmonic) terms become more significant.

4. Index modulation

We now proceed to consider the modulation of the refractive index, where $\phi(t)$ varies in time and a and σ are constant. The Neumann series solution of Eq. (8) for the transmission coefficient, $T_\phi(t)$, is

$$T_\phi(t) = \sigma - a\mathrm{e}^{-i\phi(t)} + \quad \sum_{n=1}^{\infty}\sigma^n a^n\left[\sigma - a\mathrm{e}^{-i\phi(t-n\tau)}\right]\prod_{m=0}^{n-1}\mathrm{e}^{-i\phi(t-m\tau)}. \tag{19}$$

As in the case of loss modulation, the expression for $T_\phi(t)$ consists of an instantaneous response, which is given by the first two terms, and a summation of memory terms where each preceding round-trip is weighted by σa.

#100170 - $15.00 USD Received 14 Aug 2008; revised 11 Sep 2008; accepted 16 Sep 2008; published 19 Sep 2008

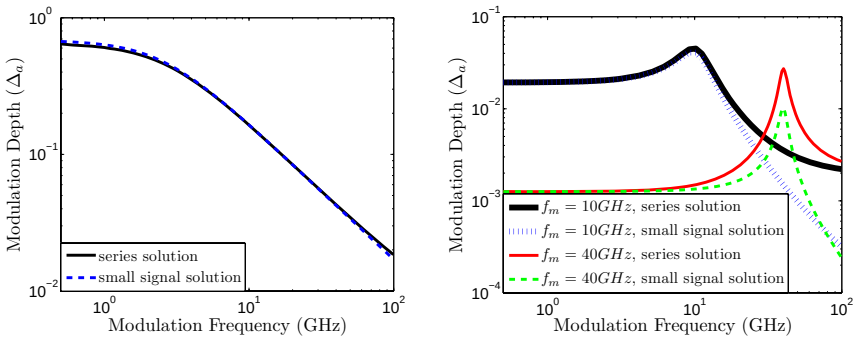

Fig. 2. Modulation depths of a microring resonator with sinusoidal loss modulation between 2 dB/cm and 5 dB/cm. $a_0 = 0.9975$, $a' = 0.0011$, and $\sigma = 0.9928$. (a): The input is on resonance. (b): Detuned input, with the modulation resonance frequency at f_m.

4.1. Small-signal approximation

Similar to Section 3.1, we shall find the small signal modulation characteristics of the resonator transmission. The round-trip phase-shift can be expressed as

$$\phi(t) = \phi_0 - \phi' \cos(\Omega_m t). \tag{20}$$

The phase-shift can be expanded into Bessel functions using the Jacobi-Anger identity:

$$e^{-i\phi(t)} = e^{-i\phi_0} \sum_{n=-\infty}^{\infty} i^n J_n(\phi') e^{in\Omega_m t}. \tag{21}$$

For $\phi' \ll 1$, only the J_0 and J_1 terms dominate and $J_0(\phi') \approx 1$ and $J_1(\phi') \approx \phi'/2$. Therefore,

$$e^{-i\phi(t)} \approx e^{-i\phi_0} + i\phi' e^{-i\phi_0} \cos(\Omega_m t). \tag{22}$$

We substitute Eq. (22) into Eq. (7) and take the Fourier transform of the resulting equation to obtain

$$\begin{aligned} &\tilde{T}_\phi(\Omega)[1 - a\sigma e^{-i(\phi_0+\Omega\tau)}] - i\frac{\phi'}{2} a\sigma e^{-i(\phi_0+\Omega\tau)} [\tilde{T}_\phi(\Omega-\Omega_m) e^{i\Omega\tau} + \tilde{T}_\phi(\Omega+\Omega_m) e^{-i\Omega\tau}] \\ &\quad = (\sigma - a e^{-i\phi_0})\delta(\Omega) - i\frac{\phi'}{2} a e^{-i\phi_0} [\delta(\Omega-\Omega_m) + \delta(\Omega+\Omega_m)]. \end{aligned} \tag{23}$$

Equation (23) can be solved to first order in ϕ'. $\tilde{T}_\phi(0) = \tilde{T}_a(0) = T_{ss}$, which is the static response of the resonator, and

$$\tilde{T}_\phi(\Omega_m) = i\frac{\phi'}{2} \frac{a e^{-i\phi_0}[\sigma \tilde{T}_\phi(0) - \delta(0)]}{1 - \sigma a e^{-i(\phi_0+\Omega_m\tau)}}, \tag{24a}$$

$$\tilde{T}_\phi(-\Omega_m) = i\frac{\phi'}{2} \frac{a e^{-i\phi_0}[\sigma \tilde{T}_\phi(0) - \delta(0)]}{1 - \sigma a e^{-i(\phi_0-\Omega_m\tau)}}. \tag{24b}$$

#100170 - $15.00 USD Received 14 Aug 2008; revised 11 Sep 2008; accepted 16 Sep 2008; published 19 Sep 2008

Finally, the modulation depth, Δ_ϕ, can be found using Eq. (15) to be

$$\Delta_\phi = 2\phi' \left[\frac{\sigma a(1-\sigma^2)\sin(\phi_0)}{\sigma^2+a^2-2\sigma a\cos(\phi_0)} \right] \times \left[\frac{1+a^4-2a^2\cos(\Omega_m\tau)}{(1-\sigma^2a^2)^2+4\sigma^2a^2[\cos(\phi_0)-\cos(\Omega_m\tau)]^2-4\sigma a(1-\sigma a)^2\cos(\phi_0)\cos(\Omega_m\tau)} \right]^{\frac{1}{2}}. \quad (25)$$

If the input is on resonance, Eq. (25) gives $\Delta_\phi = 0$. Intuitively, this is because the resonance wavelength is at the minimum of the static transmission spectrum. Thus, to first order in ϕ', there is no modulation in the transmission amplitude, and the microring operates as a phase modulator rather than an intensity modulator. As a, $\sigma \to 1$, the 3 dB roll-off frequency decreases, so the modulation bandwidth is again Q limited. By taking the derivative of Eq. (25), we find that for high Q resonators where a, $\sigma \approx 1$, a modulation resonance also exists for index modulation, with the modulation depth reaching a maximum at $\phi_0 + \Omega_m\tau \approx 2p\pi$, where p is an integer.

4.2. Numerical results

Figure 3 shows Δ_ϕ versus the modulation frequency for a sinusoidally index modulated microring resonator. The figure compares the results of the small signal modulation depth from Eq. (25) and the exact solution from Eq. (19). For the calculations, $\phi_0 = 0.039477$ and $\phi' = 0.005$, which corresponds to an index change of 2×10^{-5} at a wavelength of 1.55 μm. The two sets of calculations in Fig. 3 are identical except the values of a and σ are interchanged. The low frequency modulation depth is identical between the two cases and is therefore symmetric in a and σ, as can be seen in Eq. (25). However, at higher frequencies, the modulation depth is slightly larger for the over-coupled ($\sigma < a$) ring.

There is good agreement between the small signal approximation and the exact solution for low modulation frequencies. The modulation depth at the modulation resonance can be much greater than the low frequency modulation depth. At higher frequencies near and greater than the modulation resonance, the deviation of the small signal analysis from the series solution becomes more severe due to the presence of the higher order sidebands which can be near or on resonance at other frequencies. The presence of higher order harmonics distorts the output.

5. Coupling modulation

Finally, we consider the case where the coupling strength between the waveguide and the resonator is modulated, while a and ϕ are constant in time. The solution of Eq. (8) for $T_\sigma(t)$ is

$$T_\sigma(t) = \sigma(t) - \frac{\kappa(t)}{\kappa(t-\tau)} a e^{-i\phi} + \kappa(t) \sum_{n=1}^{\infty} \frac{a^n e^{-in\phi}}{\kappa(t-n\tau)} \left[\sigma(t-n\tau) - \frac{\kappa(t-n\tau)}{\kappa(t-(n+1)\tau)} a e^{-i\phi} \right] \prod_{m=1}^{n} \sigma(t-m\tau). \quad (26)$$

We can immediately note an important difference between Eq. (26) and Eq. (9) or Eq. (19). In Eq. (26), the memory terms embodied by the summation are multiplied by $\kappa(t)$, the instantaneous value of the coupling coefficient – such a term is absent in Eq. (9) and Eq. (19). This, as we shall further demonstrate, implies that coupling modulation does not suffer from the same limitations as loss and index modulation.

#100170 - $15.00 USD Received 14 Aug 2008; revised 11 Sep 2008; accepted 16 Sep 2008; published 19 Sep 2008

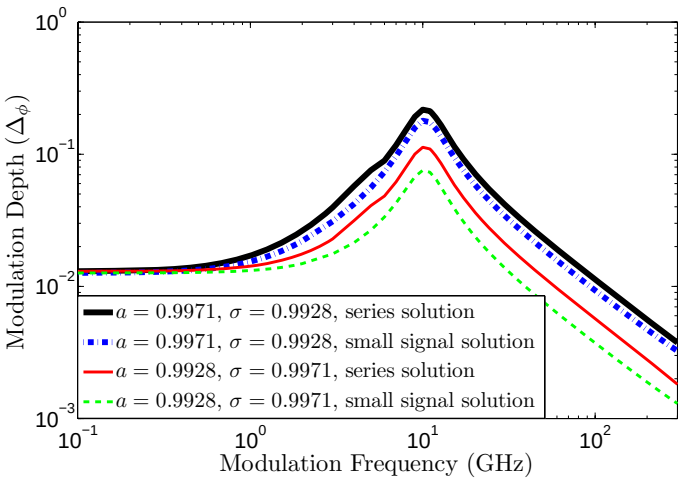

Fig. 3. Modulation depths of a microring resonator with a sinusoidal index modulation. $\phi_0 = 0.039477$ and $\phi' = 0.005$. The input is detuned from resonance, with the modulation resonance frequency at 10 GHz.

5.1. *Small-signal approximation*

We now analyze a small amplitude sinusoidal modulation of the coupling strength to obtain a simplified expression for the modulation characteristics from Eq. (26). For simplicity, we assume that the resonator is high Q, such that $\kappa \ll 1$ and $\sigma \approx 1$. We take the coupling coefficient as

$$\kappa(t) = \kappa_0 + \kappa' \cos(\Omega_m t), \tag{27}$$

where, $|\kappa'/\kappa_0| \ll 1$. For $|\sigma(t)|^2 + |\kappa(t)|^2 = 1$ to $O(\kappa')$, it follows that

$$\sigma(t) = \sigma_0 + \sigma' \cos(\Omega_m t), \tag{28}$$

where $\sigma' = -\kappa_0\kappa'/\sigma_0$ and $|\sigma'/\sigma_0| \approx \kappa'\kappa_0$. Substituting Eq. (27) and (28) into Eq. (7) up to $O(\kappa')$, and taking the Fourier transform results in

$$\begin{aligned}
&\kappa_0 \tilde{T}_\sigma(\Omega)[1 - a\sigma_0 e^{-i(\phi+\Omega\tau)}] + \frac{\kappa'}{2}\tilde{T}_\sigma(\Omega-\Omega_m)\left[e^{-i\Omega_m\tau} - ae^{-i(\phi+\Omega\tau)}\left(\sigma_0 e^{i\Omega_m\tau} - \frac{\kappa_0^2}{\sigma_0}\right)\right] \\
&\quad + \frac{\kappa'}{2}\tilde{T}_\sigma(\Omega+\Omega_m)\left[e^{i\Omega_m\tau} - ae^{-i(\phi+\Omega\tau)}\left(\sigma_0 e^{-i\Omega_m\tau} - \frac{\kappa_0^2}{\sigma_0}\right)\right] \\
&\quad = \kappa_0[\sigma_0 e^{-i\Omega\tau} - ae^{-i\phi}]\delta(\Omega) + \frac{\kappa'}{2}\left(\sigma_0 e^{-i\Omega\tau} - \frac{\kappa_0^2}{\sigma_0}e^{-i(\Omega-\Omega_m)\tau} - ae^{-i\phi}\right)\delta(\Omega-\Omega_m) \\
&\quad + \frac{\kappa'}{2}\left(\sigma_0 e^{-i\Omega\tau} - \frac{\kappa_0^2}{\sigma_0}e^{-i(\Omega+\Omega_m)\tau} - ae^{-i\phi}\right)\delta(\Omega+\Omega_m).
\end{aligned} \tag{29}$$

We can solve for $\tilde{T}_\sigma(0)$, $\tilde{T}_\sigma(\Omega_m)$, and $\tilde{T}_\sigma(-\Omega_m)$ in the same fashion as was done for index and loss modulation. To $O(\kappa')$, $\tilde{T}_\sigma(0) = T_{ss}$, the static response of resonator. Using Eq. (15) to solve for the modulation depth, we obtain

$$\Delta_\sigma = 2\sigma' \left| \frac{(1-a^2e^{-i\Omega_m\tau})[\sigma_0 - a\cos\phi + a\sigma_0(a-\sigma_0\cos\phi)e^{-i\Omega_m\tau}]}{(\sigma_0^2 + a^2 - 2a\sigma_0\cos\phi)(1 + a^2\sigma_0^2 e^{-2i\Omega_m\tau} - 2a\sigma_0\cos\phi e^{-i\Omega_m\tau})} \right|. \tag{30}$$

#100170 - $15.00 USD Received 14 Aug 2008; revised 11 Sep 2008; accepted 16 Sep 2008; published 19 Sep 2008

To simplify Eq. (30), we take the input wavelength exactly on resonance, such that $\exp(i\phi) = 1$, and $\Omega_m \tau \ll 1$ to arrive at

$$\Delta_{\sigma,res} = 2\sigma' \left[\frac{(1-a^2)^2 + a^2(\Omega_m \tau)^2}{(\sigma_0 - a)^2 \left[(1-a\sigma_0)^2 + a\sigma_0(\Omega_m \tau)^2\right]} \right]^{\frac{1}{2}}. \tag{31}$$

Equation (31) shows that the frequency response of the modulator depends strongly on the relative magnitudes of a and σ_0. At low modulation frequencies, $\Omega_m \tau \ll (1-a\sigma_0)/\sqrt{a\sigma_0}$, $\Delta_{\sigma,res}$ is approximately constant and equal to $2\sigma'(1-a^2)/[|\sigma_0 - a|(1-a\sigma_0)]$. At high frequencies such that $\Omega_m \tau \gg (1-a\sigma_0)/\sqrt{a\sigma_0}$, the modulation depth is also constant and equal to $2\sigma'\sqrt{a/\sigma_0}/|\sigma_0 - a|$. Thus, there is no frequency roll-off to the modulation depth.

5.2. Numerical results

Figure 4 compares the modulation depths for resonant and detuned inputs of two sinusoidally coupling modulated microring resonators: one under-coupled and the other over-coupled. The loss of the rings is taken to be 4 dB/cm, $a = 0.9971$. The series solutions, Eq. (26), closely follow the predictions of Eqs. (30) and (31). The low frequency modulation depth is smaller than the high frequency value for over-coupled ring resonators and vice-versa for under-coupled resonators. In addition, the results show that for both resonant and detuned inputs, the modulation depth is roughly constant at large frequencies. However, comparing Fig. 4 (a) with Fig. 4 (b), we can see that the input wavelength should be close to resonance to achieve large modulation depths. Fig. 4 (b) also shows the existence of modulation resonance for coupling modulation with the input detuned from resonance.

We can understand the modulation characteristics by examining the amplitude of the waves that interfere to produce the output, $B(t)$, in Fig. 1. The modulation of the coupling constant, similar to index or loss modulation, generates frequency sidebands to the input frequency, ω_0, that also circulate in the microring. The amplitude of these sidebands diminish with increasing modulation frequency or increasing Q, which leads to the roll-off in the modulation depth for index and loss modulation. In contrast, for coupling modulation, as can be seen in Eq. (26), a factor of $\kappa(t)$ is applied to any light that exits the cavity. Therefore, the output of the modulator is determined by the instantaneous modulation of the frequency components at ω_0 and the sidebands.

At low modulation frequencies, both the sidebands and ω_0 components are modulated simultaneously. However, there will be a modulation frequency range over which the sideband amplitudes diminish, leaving only the instantaneous modulation of ω_0, which is independent of modulation frequency. The flat high frequency modulation responses in Fig. 4 are due to this instantaneous modulation. The higher the Q factor is, the lower the modulation frequency needs to be for the modulator to reach the flat high frequency response, i.e. $\Omega_m \tau \gg (1-a\sigma_0)/\sqrt{a\sigma_0}$ in Eq. (31). It is as though there is a "low frequency limit" to the operation of the coupling-modulated microring.

6. Discussion

Intuitively, we may understand the lack of a modulation frequency roll-off for coupling modulation as follows. Consider the static scenario in which a CW wave is input to the microring. Initially, $\kappa \neq 0$, which results in a certain transmission amplitude. If κ is suddenly reduced to zero, immediately, no light can exit or enter the resonator. This leads to an instantaneous change in the transmission that is not limited by the resonator Q, but only the response of the coupler. On the other hand, if the loss or index of the resonator is changed suddenly, light that was circulating inside the resonator can continue to escape from the resonator. The rate at which

#100170 - $15.00 USD Received 14 Aug 2008; revised 11 Sep 2008; accepted 16 Sep 2008; published 19 Sep 2008

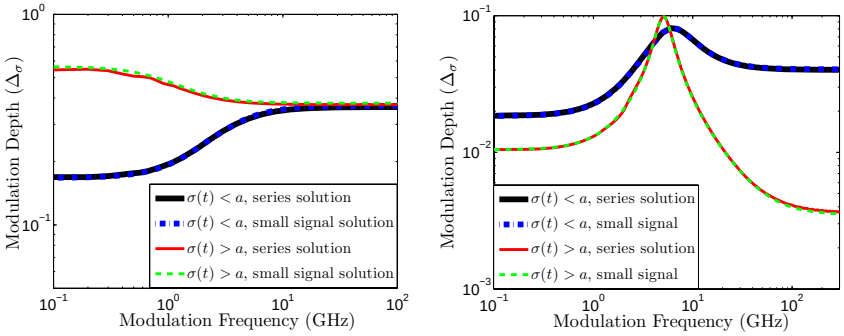

Fig. 4. Modulation depths of a microring resonator with a sinusoidal modulation of the coupling strength. Over-coupled: $\sigma' = 0.0013$ and $\sigma_0 = 0.9902$. Under-coupled: $\sigma' = 3.5 \times 10^{-4}$ and $\sigma_0 = 0.999$. The loss of the ring is 4 dB/cm, $a = 0.9971$. (a): The input is on resonance. (b): The input is detuned from resonance, with the modulation resonance frequency at 5 GHz.

the amplitude of the light in the resonator decays is inversely proportional to the Q factor. In the steady-state intensity transmission, Eq. (6b), σ and a are interchangeable. Therefore, a static description of the resonator would not distinguish between changes in a and σ. It is only through a dynamical description of the resonator that the differences in the modulation rate limits can be revealed.

To further illustrate the difference between coupling modulation and index/loss modulation, we shall briefly examine a "large" modulation of the input CW wave. Due to the complicated nature of the interference that occurs at the output when device parameters are modulated, it is unlikely that the output from an arbitrary modulation waveform would simply be a superposition of the small signal sinusoidal outputs presented earlier.

Figure 5 illustrates the outputs attainable with a Gaussian pulse modulation of the index, loss, and coupling calculated using Eqs. (9), (19), and (26). The full-width half-maximum widths of the modulating pulses are 42 ps, 21 ps, and 8 ps. The output pulses generated from loss and index modulation suffer from distortion and time delays relative to the modulation waveform, which are considerably worse for smaller pulse widths. In addition, the amplitudes of the output pulses decrease significantly with shorter index or loss pulse widths.

In contrast, the output pulses in Fig. 5(f) generated from coupling modulation do not decrease in amplitude with shorter modulation pulse widths. However, the output pulses are shorter than the modulation pulses in Fig. 5(c). This distortion is due to the low frequency limit of a coupling modulated microring resonator suppressing the tails of the Gaussian pulse. The Q of the resonator must be very large to produce pulses that closely resemble the coupling strength pulse shape. This is the opposite requirement compared to loss or index modulation which suffer from high frequency limitations and thus require low Q resonators for undistorted output pulses.

The modulation depth does not remain constant at arbitrarily high modulation frequencies of the coupling strength. If the device parameters are modulated with a periodicity of τ in Eq. (7), the resonator output is identical to the low frequency response, neglecting any averaging of device parameters that occur as a result of Eq. (1). Therefore, the response of a coupling modulated microring resembles the low frequency response at modulation frequencies approaching

#100170 - $15.00 USD Received 14 Aug 2008; revised 11 Sep 2008; accepted 16 Sep 2008; published 19 Sep 2008

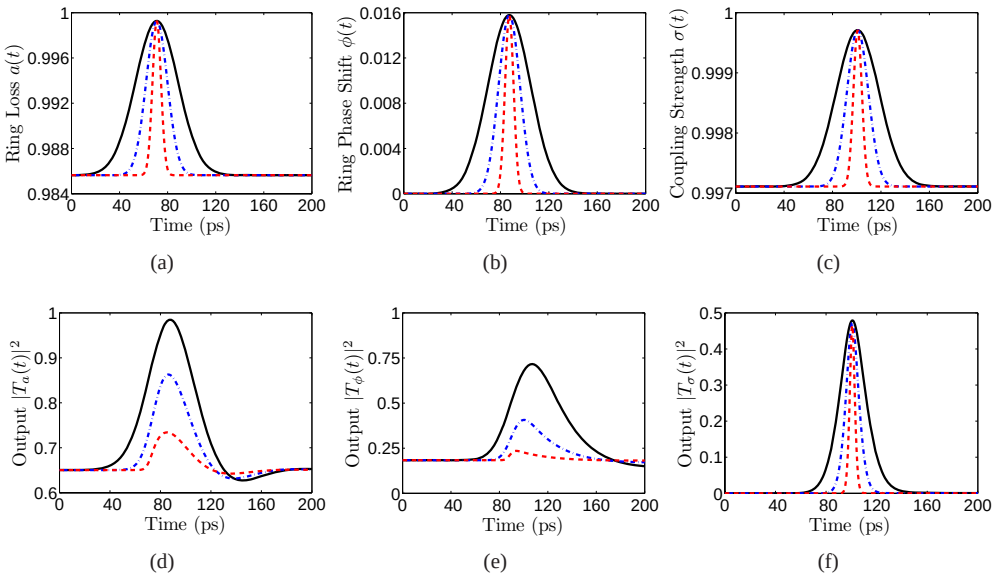

Fig. 5. Device parameters (top) and the corresponding output intensities (bottom) versus time for single-pulse modulated microring resonators. (a), (d): Loss modulation, $\sigma = 0.9928$, and the input is resonant. (b), (e): Index modulation, $\phi_0 = 0.039477$, $\sigma = 0.9928$, and a loss of 4 dB/cm. (c), (f): Coupling modulation, the loss is 4 dB/cm, and the input is resonant.

the FSR of the resonator. However, for microring resonators, the FSR is on the order of ~ 1 THz, sufficient for most communication applications. Moreover, throughout this analysis, we have neglected the frequency, amplitude, and phase response of the coupler itself. The ultimate modulation rate would be determined by the modulation response of the coupler, which need not be a resonant device. For example, state-of-the-art electro-optic polymer Mach-Zehnder interferometric switches can operate at > 100 GHz [15, 16].

The main advantage of a resonant modulator is that in contrast to its non-resonant counterpart, only very small changes in the device parameters are required for a high extinction ratio. In Fig. 5(f), the change in κ is only of the order of 10^{-3}, i.e. the loaded Q is almost constant. Therefore, a high Q, microring modulator based on variable coupling can still be low power and compact in size. Recently, microrings integrated with a variable coupler have been proposed and demonstrated [17]-[22]. Those with non-resonant couplers, similar to the configurations presented in [17]-[20], would appear to be the most promising for ultra-high speed operation.

7. Conclusion

In summary, we have presented a dynamical analysis of a microring modulator in which the loss, index, or waveguide-ring coupling strength is modulated. We extended our fully rigorous results to small signal approximations to show that when the waveguide-ring coupling coefficient is modulated, the modulation bandwidth of the microring approaches the FSR. We compared pulse modulation of the loss, index, and coupling strength, to find that variable coupling is the most promising for generating short pulses with minimal distortion. Coupling modulation has the potential of leveraging the resonant nature of high Q microresonators to realize low loss, low power, and compact modulators which also possess a high modulation bandwidth.

#100170 - $15.00 USD Received 14 Aug 2008; revised 11 Sep 2008; accepted 16 Sep 2008; published 19 Sep 2008

Our model can be extended to incorporate the dynamic effects of the coupler and to analyze other properties of microring modulators, such as the chirp, linearity, and extinction ratio.

Acknowledgments

The support of the Natural Sciences and Engineering Research Council of Canada is gratefully acknowledged.

#100170 - $15.00 USD Received 14 Aug 2008; revised 11 Sep 2008; accepted 16 Sep 2008; published 19 Sep 2008